Biogeosciences Discuss., doi:10.5194/bg-2016-204, 2016
Manuscript under review for journal Biogeosciences
Published: 18 July 2016

Archive of bacterial community in anhydrite crystals from a deep-sea basin provides evidence of past oil-spilling in a benthic environment in the Red Sea

Yong Wang[1,2], Tie Gang Li[3,4], Meng Ying Wang[1], Qi Liang Lai[5], Jiang Tao Li[6], Zhao Ming Gao[1], Zong Ze Shao[5], Pei Yuan Qian[2,*]

[1]Institute of Deep-Sea Science and Engineering, Chinese Academy of Sciences, San Ya, China

[2] Division of Life Science, Hong Kong University of Science and Technology, Clear Water Bay, Hong Kong, China

[3] Key Laboratory of Marine Sedimentology and Environmental Geology, First Institute of Oceanography, State of Oceanic Administration (SOA), Qingdao, China

[4]Laboratory for Marine Geology, Qingdao National Laboratory for Marine Science and Technology, Qingdao, China

[5] Key Laboratory of Marine Biogenetic Resources, The Third Institute of Oceanography, SOA, Xiamen, China

[6] State Key Laboratory of Marine Geology, Tongji University, Shanghai, China

***Corresponding author:** boqianpy@ust.hk, Tel: 852-2358-7331

Keywords: *Alcanivorax*; metagenome; anhydrite; Atlantis II brine pool; hydrothermal sediment

Running title: Archive of microbial inhabitants in anhydrites

Biogeosciences Discuss., doi:10.5194/bg-2016-204, 2016
Manuscript under review for journal Biogeosciences
Published: 18 July 2016

Abstract

In deep-sea sediment, the microbes present in anhydrite crystals after mild hydrothermal activities are markers of the past environment. In this study, this hypothesis was tested by analyzing the metagenome of an anhydrite crystal sample from a hydrothermal and hypersaline sediment core sampled from the Atlantis II Deep in the Red Sea. The 16S/18S rRNA genes in the metagenome were assigned to Bacteria, Archaea, Fungi and even invertebrate species. The dominant species in the crystals was an alkane-degrading *Alcanivorax* bacterium, which was not detected in the adjacent sediment layer. Using a genome-binning method, a draft genome of the *Alcanivorax* bacterium was separated from the metagenome. Phylogenetic and genomic analyses revealed that this species was a close relative of *Alcanivorax borkumensis* Sk2. The draft genome contained all the functional genes for alkane utilization and the reduction of nitrogen oxides. Fluorescence microscopy using 16S rRNA and marker gene probes revealed intact cells of the *Alcanivorax* bacterium in the crystals. Moreover, the metagenomes of the anhydrites and control sediment contained aromatic degradation pathways, which were mostly derived from *Ochrobactrum* sp. The estimated age of the anhydrite layer was between 750-770 years, which might span the event of hydrothermal eruption into the benthic floor. Altogether, these results support the presence of an oxic, oil-spilling benthic environment in the Atlantis II basin of the Red Sea in approximately the 14th century. The original microbial inhabitants underwent a dramatic selection process via drastic environmental changes following the formation of an overlying anoxic brine pool in the basin due to hydrothermal activities.

Biogeosciences Discuss., doi:10.5194/bg-2016-204, 2016
Manuscript under review for journal Biogeosciences
Published: 18 July 2016

1. Introduction

Deep-sea sediment is among the least explored biospheres on Earth. Indigenous microbes differ vastly in community composition and metabolic spectra at different depths and sites [1,2]. The distribution of microbes in subsuperficial sediments is determined by the porosity, nutrient availability and geochemical conditions of the sediment [3,4]. Variations in these parameters in sediment layers lead to the stratification of microbial communities. In return, genomic features and the community composition of the indigenous microbial inhabitants may reflect the *in situ* conditions. However, dead microbes cannot be well preserved and will be degraded by biological and abiological activities. Most of the biological markers containing the geochemical indicators were lost due to lack of preservation processes. Although lipids and other organic carbons present in some minerals allow the prediction of microbial activities to some extent [5], the original metabolic activities have been difficult to retrieve in a comprehensive and precise manner.

Although most of the dead microbes are damaged during the sedimentation process, some likely can be maintained in almost their original shape. Evaporites, which mostly consist of halite and anhydrite ($CaSO_4$) or gypsum ($CaSO_4 \cdot 2H_2O$, temperature <38℃ [6]), are common microbialites with accretionary organosedimentary structures [7]. Numerous dead bacteria, algae and metazoans have been detected in gypsum granules [8,9]; bacterial mats growing on evaporites may become trapped and constitute much larger microbialites [10]. Consequently, microbial inhabitants on the benthic surface become trapped in the evaporites. Anhydrite facies are not found throughout deep-sea sediments. They usually form around hydrothermal vents in deep-sea environments [11]. A strong deep-sea volcanic eruption may break the crustal basalts, resulting in a drastic emission of hydrothermal gases followed by the crystallization of anhydrites and the deposition of metal sulfides [12]. An alternative model is that mild hydrothermal activities lead to a slow influx of solutions into the overlying sediment at temperatures in the sub-seafloor ranging from 20-100℃. This process also results in the formation of crystalline anhydrites in veins and around warm vents [11]. The latter process may trap microbial inhabitants on the seafloor and within surface layers in anhydrites. Due to the mild temperature, the trapped bodies are better preserved as excellent biological markers that contain hints of past geochemical conditions.

Biogeosciences Discuss., doi:10.5194/bg-2016-204, 2016
Manuscript under review for journal Biogeosciences
Published: 18 July 2016

A similar geological setting is present in the Red Sea. Initially located in a deep-sea rift in the 1960s [13,14], the temperature of the Atlantis II brine pool has recently increased to 68℃ [15]. In 1972, several sediment cores were obtained from the southwest region of the pool (DSDP Site226), and metal sulfides and evaporites were recognized as major mineral facies in this brine-filled basin [16]. In particular, thick and well-crystalized anhydrite layers were found within the hematite and at the bottom of the cores. Two major anhydrite units were later defined by analysis of the adjacent core samples. The lower unit comprised anhydrite ranging from 12 to 70 wt% [17]. The anhydrite in the sediments likely resulted from a geyser-type eruption of hydrothermal solutions into the Atlantis II brine pool followed by the mixing of calcium-rich solutions with dissolved sulfate-bearing brine and the precipitation of anhydrites during the cooling process [18]. The discovery of veins containing sulfides and anhydrite in the sediment suggests that a mild hydrothermal eruption created the anhydrite facies in the Atlantis II sediment [19-21]. The formation of anhydrite facies in this manner would trap microbial cells and organic debris in the bottom water and surface sediment. Hence, these anhydrite layers probably contained important indigenous microbial inhabitants during the occurrence of the hydrothermal events at the deep-sea benthic floor of the Red Sea. Coupled with other markers to estimate age, the anhydrite facies probably contained a large quantity of information regarding the past geochemical changes.

In the present study, we sampled a sediment core near Site226 and detected an anhydrite layer. Microbial DNA was extracted from the crystals and sequenced for the metagenomic study. The dominant species were alkane- and oil-degrading bacteria, together with some archaeal species. In contrast, the microbial community residing in the neighboring control sediment differed substantially from that in the anhydrite crystals. The present study sheds light on the importance of anhydrites in deep-sea sediment as an archive of microbial inhabitants that can serve as biomarkers of past geochemical events.

2 Materials and methods

2.1 Physicochemical measurements of sediment layers

Biogeosciences Discuss., doi:10.5194/bg-2016-204, 2016
Manuscript under review for journal Biogeosciences
Published: 18 July 2016

In 2008, a 2.25-meter gravity sediment core was obtained from the southwest basin (approximately 2180 meters below sea level) of the Atlantis II Deep (21°20.76' N, 38°04.68' E) in the Red Sea [22]. The core was frozen at -80℃ and then sliced aseptically into seventy-five 3-cm sections. Microbes from sediment slices of 12-15 cm, 63-66 cm, 105-108 cm, 183-186 cm, and 222-225 cm were first suspended in phosphate-buffered saline and shaken on a vortexer for 30 s. The supernatant was filtered through a 0.22-μm black polycarbonate filter. After 6-diamidino-2-phenyloindole (DAPI) staining, the microbes from each layer were counted under an epifluorescence microscope (n = 3) [23]. The pore water from the above 5 layers was collected by centrifugation. The concentration of dissolved organic carbon (DOC) in the pore water was determined using the combustion method [9]. The concentrations of ammonium, nitrite and nitrate were measured using a TNM-I analyzer (Simadzu, Kyoto, Japan). To separate large particles (>63 μm) from small particles (<63 μm), the sediment samples were passed through a 63-μm stainless steel sieve. The percentage of small particles (dry weight) was calculated for all slices.

The age of the sections was estimated with a radiometric dating method that utilizes the naturally occurring radioisotope ^{14}C. The monospecific *Globigerinoides sacculifer* specimens ranging in size from 250 to 350 μm were manually selected with caution and then subjected to ^{14}C measurement in the National Ocean Sciences Accelerator Mass Spectrometry (AMS) Facility at the Woods Hole Oceanographic Institute, USA. The raw AMS ^{14}C ages were converted to calendar ages using the CALIB 6.0 program (http://calib.qub.ac.uk/calib/) with the dataset Marine 09 [24]. A reservoir correction has been considered for the ^{14}C difference between atmospheric and surface waters [25].

2.2 DNA extraction and amplification

The boundary of the anhydrite layer was determined by naked eye observation and particle size measurement. Crystals were manually collected from the layers, followed by ultrasonic cleaning. The grounded crystals were then analyzed by X-ray diffraction (XRD) (Rigaku, Tokyo, Japan) using Cu Ka radiation of 40 kV and 30 mA. The following procedure was conducted for DNA extraction from the crystals with caution to avoid contamination. Surface contamination was removed by rinsing with 70% alcohol in

Biogeosciences Discuss., doi:10.5194/bg-2016-204, 2016
Manuscript under review for journal Biogeosciences
Published: 18 July 2016

autoclaved distilled deionized water, followed by pulsed ultrasonic cleaning for 2 hours. Anhydrite crystals (20 g) (Fig. 1A) of different sizes were treated with 1 μL (2U) Turbo DNase I (Ambion, Austin, Texas, US) for 30 m in a 37℃ incubation before being ground for DNA extraction in a sterile hood. The anhydrite powder was used for DNA extraction with the PowerSoil DNA Isolation kit (MO-BIO, Carlsbad, USA), followed by a purification step according to the manufacturer's instructions. Twenty picograms of the raw DNA extract was used for DNA amplification using a MALBAC kit (Yikang, Jiangsu, China) according to the manufacturer's manual [26]. The MALBAC amplification method has been evaluated recently in metagenomic studies [27]. Two MALBAC amplification assays were conducted using twenty-one PCR cycles to acquire a sufficient amount of DNA for subsequent sequencing. A negative control was also incorporated in the assay. The DNA concentration of the MALBAC-amplified sample and the negative control was measured with a Bioanalyzer (Agilent, CA, US). The products of the MALBAC amplification and negative control were examined by gel electrophoresis to validate the size ranges of the amplicons. Three replicates of MALBAC amplifications for each sample were mixed and used for Illumina sequencing on a Hiseq2500 platform. As a control, 10 g of sediment from a position at 168 cm from the top of the core was used for DNA extraction. There were no recognizable anhydrite crystals in this layer. DNA amplification and sequencing were conducted as described above.

2.2 Binning of metagenomes

The initial Illumina 2×110-bp paired-end reads were subjected to quality assessments using the NGS QC Toolkit with default parameters (Patel and Jain, 2012). The Illumina sequencing data were deposited in the NCBI SRA database (accession number SRA356974). The 35-bp MALBAC adapters at the start of the sequencing reads were removed. Assembly of the trimmed Illumina 2×75-bp paired-end reads was performed using SPAdes 3.5 [28]. The read coverage for the assembled contigs was calculated using SAMtools [29]. The 16S/18S rRNA genes in the contigs were identified using rRNA_HMM [30]. Taxonomic sorting of the 16S rRNA genes was conducted in the SILVA database with a confidence threshold of 80%. The relative abundance of the species in the metagenomes was roughly estimated based on the coverage of the 16S/18S rRNA genes. Binning of the

Biogeosciences Discuss., doi:10.5194/bg-2016-204, 2016
Manuscript under review for journal Biogeosciences
Published: 18 July 2016

draft genomes was performed based on the read coverage and G+C content of the contigs (Fig. 1B), followed by principal component analysis (PCA) of the tetranucleotide frequencies (TNF) of their respective contigs using a previously described pipeline (Fig. 1C) [31]. The binning process was visualized with the RStudio program (https://www.rstudio.com). To evaluate the completeness of the draft genome, conserved single-copy genes (CSCGs) were counted in the genome. The CSCGs were identified by searching the CDSs against an HMM database of essential bacterial genes (107 essential genes) [31] using hmmsearch (3.0) with default cutoffs for each protein family.

2.3 Genomic analyses

The coding DNA sequences (CDSs) of the draft genome were predicted using Prodigal (version 2.60)[32]. KEGG annotation of the CDSs was performed using BLASTp against the KEGG database [33] with a maximum e-value cutoff of 1e-05. The KEGG pathways were reconstructed using the KEGG website (http://www.kegg.jp). CDSs were also annotated against the NCBI NR database, and MEGAN was used for taxonomic affiliation and SEED/subsystem annotation of the CDSs [34]. The draft genome was submitted to NCBI (accession number LKAP00000000). The average nucleotide identity (ANI) was calculated using the algorithm integrated in the web service of EZGenome [35]. The DNA-DNA hybridization (DDH) estimate value was calculated using the genome-to-genome distance calculator (GGDC2.0) with the alignment method of BLAST+ [36-38].

2.4 Detection and phylogeny of 16S ribosomal RNA (rRNA) genes

The 16S rRNA gene sequence was identified from the draft genome sequence. The closest relatives based on 16S sequence similarity were determined using the web service of EzTaxon [39]. The neighbour-joining phylogenetic tree was constructed using MEGA version 5.0 [40] with the Kimura 2-parameter model. The phylogenetic tree was supported with bootstrap values based on 1000 replications.

2.5 Fluorescence *in situ* hybridization (FISH) of *Alcanivorax* bacteria

FISH probes for *Alcanivorax* bacteria were designed using the 16S rRNA gene extracted from the *Alcanivorax* draft genome. Two 16S rRNA fragments, 5'-

Biogeosciences Discuss., doi:10.5194/bg-2016-204, 2016
Manuscript under review for journal Biogeosciences
Published: 18 July 2016

CCTCTAATGGGCAGATTC-3' and 5'-CCCCCTCTAATGGGCAGA-3', were selected as candidate probes with Probe_Design in the ARB package [41]. The coverage efficiency of the probes was then examined in the Silva database [42]. The 6-FAM-labeled probe used to target the *alkB* gene was 5'-ATGGAGCCTAGATAATGAAGT-3' [43]. A pure culture of *Alcanivorax borkumensis* Sk2 was first used to examine the probes before performing the assay. Two grams of anhydrite crystals were sonicated for 30 min in 1 U DNase I solution. The crystals were washed with deionized water and then ground into a powder with a beadbeater in a germ-free environment. The supernatant was mixed with 37% formaldehyde (final concentration, 1-4%). To fix the cells in PBS buffer, the sample was maintained at 4℃ for 3-4 hr. After centrifugation at 13,000 r/min for 3 min, the supernatant was discarded. The remaining microbes were soaked in 200 μL of PBS buffer, followed by addition of 200 μL of ethanol [44]. The sample was filtered through 3-μm and 0.22-μm membranes sequentially (diameter, 25 mm; Millipore, Eschborn, Germany). After dehydration of the membrane using alcohol, 2 μL of dying solution containing oligonucleotide probes and 20 μL of buffer (360 μL of 5 M NaCl，40 μL of 1 M Tris/HCl，700 μL of 100% formamide，2 μL of 10% SDS，and water to a total volume of 2 mL). The hybridization of the probes to the microbes was performed for 2 h at 46℃. Rinsing buffer (700 μL of 5 M NaCl, 1 mL of 1 M Tris/ HCl, 500 μL of 0.5 M EDTA, 50 μL of 10% SDS and water to a total volume of 50 mL) was used to remove free probes. For counterstaining, 50 μL of 4', DAPI solution (1 μg/mL) was added to the sample. After incubation for 3 min, the sample was washed in MQ (MetaPhor Bioproducts, Rockland, Maine) and 96% ethanol for 1 min [44]. The microscopic observation was conducted using an Olympus BX51 (Olympus, Tokyo, Japan).

3 Results

3.1 Physicochemical profile and cell counts

A thick anhydrite layer was present at the bottom of the sediment core based on naked-eye observation of the color and grain size. The anhydrite layer at depths ranging from 177-198 cm consisted of coarse, agglutinated crystals, which corresponded to the high percentage of large grains (78 wt% larger than 63 μm) (Fig. 2). The XRD analysis further confirmed that the crystals in this layer were anhydrite. In contrast, halite comprised the

Biogeosciences Discuss., doi:10.5194/bg-2016-204, 2016
Manuscript under review for journal Biogeosciences
Published: 18 July 2016

evaporites at depths of 12 cm, 63 cm, 105 cm and 222 cm. For the samples at different depths, the DOC concentration was measured, and the highest value was recorded at 183 cm (80.9 mg L^{-1}), which was even higher than the surface layer at 12 cm (Fig. 3). In the 12 cm layer, the cell density was 3.2×10^5 cells per cm^3, whereas in the layers at 63 cm, 105 cm and 222 cm, it was reduced by 88%, 92% and 96%, respectively (Fig. 3). The cell density was also calculated as the number of cells per gram of sediment. The results revealed a value of 7.1×10^5 cells per gram at a depth of 12 cm, which declined more than 70% in the deeper layers. Although the cell density in the 183 cm layer (6.7×10^4 cells/cm^3) was markedly lower than that in the 12 cm layer, it was higher than those in the 105 cm and 222 cm layers.

The sediment as a whole is a highly reductive environment, as indicated by the low nitrate, low nitrite and extremely high ammonium concentrations (Fig. 3). To determine the time of the anhydrite layers at 177-198 cm, an age estimate was performed for several layers. The sediment ages were estimated based on the radioisotope ^{14}C of *G. sacculifer* assuming a linear increment from the top (Fig. 2). The results obtained for the layers above and below the anhydrite layer indicated a narrow range of 750-770 years between 153 cm and 198 cm (Table 1).

3.2 Draft genome of the dominant bacterial species in anhydrites

DNA was extracted from the anhydrite crystals and the adjacent layer separately. After amplification, about 16 Gbp Illumina sequencing data were obtained and then assembled. The size of the anhydrite and control metagenomes was 59 and 84 Mbp, respectively, after assembly. The microbial communities differed remarkably according to the taxonomic assignment of the 16S/18S rRNA gene fragments in the two metagenomes (Fig. 4). At the genus level, only *Ochrobactrum* and *Alkanindiges* were common inhabitants in both samples. *Alcanivorax* and *Bacillus* were also dominant genera in the anhydrite and the control, respectively. At the phylum level, excluding the Proteobacteria, the two metagenomes had distinctive phyla. The anhydrite contained Archaea that were represented by the methanogenic *Methanoculleus* [45]; and Fungi that consisted of the Ascomycota. In contrast, the control sediment contained mainly Firmicutes, Bacteroides,

Biogeosciences Discuss., doi:10.5194/bg-2016-204, 2016
Manuscript under review for journal Biogeosciences
Published: 18 July 2016

Actinobacteria, and Deinococcus-Thermus. Surprisingly, an invertebrate species, *Prototritia* sp. belonging to Arthropoda, was identified in the anhydrite.

3.3 Genome binning of an *Alcanivorax borkumensis* genome

The binned draft genome from the anhydrite metagenome was 3,069,971 bp and comprised 77 contigs. A partial 16S rRNA gene sequence (805 bp) was extracted from the draft genome. Because the sequence was almost identical to that of *A. borkumensis* Sk2 (99.9%), we considered the binned draft genome to be from a strain of *A. borkumensis*. As shown in Figure 5, a phylogenetic tree based on the 16S rRNA gene sequences of the genus *Alcanivorax* indicated that the strain clustered with *A. borkumensis* Sk2, an exclusive and ubiquitous hydrocarbon-degrading bacterium [46,47]. The strain name of the *A. borkumensis* in the sediment core was ABS183. The coverage levels of the contigs ranged from 100-fold to 200-fold (Fig. 1B). Due to its highest level of coverage in the metagenome, *A. borkumensis* ABS183 was probably the most dominant species in the anhydrite crystals. It was the only microbial species that could be reliably separated from the metagenome.

The genome of *A. borkumensis* ABS183, despite containing gaps, was slightly smaller than that of *A. borkumensis* Sk2 (accession number NC_008260; 3,120,143 bp), suggesting that the draft genome of *A. borkumensis* ABS183 was nearly complete. The identification of a complete list of single-copy genes also supported the completeness of the genome. The DDH estimation between *A. borkumensis* ABS183 and Sk2 was 97.1%±1.3%, which was higher than the standard cut-off value of 70% for genome relatedness between pairs of species [48]. The ANI value between ABS183 and Sk2 was 99.9%, which was also higher than the standard ANI criterion for species identity (95%–96%) [49]. These results further confirmed that ABS183 was a strain of *A. borkumensis*.

The genome of *A. borkumensis* ABS183 contains two copies of the alkane-1 monooxygenase gene (*alkA*; 10502_28 and 2890_35), which is an essential functional gene for alkane utilization by *Alcanivorax* bacteria [46]. Neighboring the *alkA* genes, *alkBGHJ* genes, a GntR family transcriptional regulator gene, and a rubredoxin gene were identified. The gene order of the related genes was consistent with that of the homologs in the genome

Biogeosciences Discuss., doi:10.5194/bg-2016-204, 2016
Manuscript under review for journal Biogeosciences
Published: 18 July 2016

of strain Sk2 [46]. The *alk* genes were completely absent from the control metagenome. Moreover, the genome of *A. borkumensis* ABS183 contains genes responsible for the reduction of nitrogen oxides (KEGG genes: K00370-K00374 and K00362-K00363; nitrate reductase I genes and nitrite reductase genes). The reduction process was believed to generate ammonia for the efficient synthesis of amino acids [46]. A high demand for fatty acids was a characteristic of *A. borkumensis* to perform rapid energy and organic carbon storage. *A. borkumensis* ABS183 was probably able to synthesize long fatty acids because the *fas* and *fabBFGIKZ* genes responsible for the elongation of fatty acids were all present in its draft genome. In contrast, the essential *fas* gene (K11533) and other relevant genes were not found in the control metagenome. Crude oil generally contains aromatic compounds, and the current sediment at the sampling site also contained oil [50]. As expected, the two metagenomes possessed a complete set of genes responsible for the degradation of aromatic compounds. Based on the homology of the genes, the *Ochrobactrum* and *Alkanindiges* species probably played a role in this degradation.

3.4 Detection of bacteria in anhydrite crystals by DAPI and FISH

To determine whether complete microbial cells could be maintained in the anhydrite crystals, DAPI and FISH assays were conducted to visualize the microbes. The DAPI results revealed the presence of complete cells that were released or embedded in the crystals (Fig. 6A, D, and H). However, the FISH assay, which was used to detect *A. borkumensis* ABS183 with two probes specific to the 16S rRNA gene, showed some fluorescence-labeled microbes (Fig. 6B, E and I). These microbes could also be envisioned with the FISH assay using the *alkB* gene probe (Fig. 6F and 6J). The *alkB* is one of the functional genes that participate in alkane degradation [46]. The rod shape of the fluorescent microbes is consistent with the microscopic features reported previously [47]. These results indicated that some microbes in the microscopic fields were *A. borkumensis* ABS183, as revealed in the anhydrite metagenome.

4 Discussion

In the present study, we detected complete microbial cells and analyzed their metagenome in the anhydrite crystals from a deep-sea anoxic basin. The dominant bacterial species was

Biogeosciences Discuss., doi:10.5194/bg-2016-204, 2016
Manuscript under review for journal Biogeosciences
Published: 18 July 2016

A. borkumensis ABS183, an aerobic bacterium that is capable of degrading alkanes in crude oil. *Alcanivorax* is one of the bacterial indicators for the spilling of oil in waters and surface sediment [51]. However, the Atlantis II brine pool is anaerobic and increasingly hydrothermal [52]. The brine sediment in the basin was also found to be anoxic. Thus, *A. borkumensis* ABS183 could not be current inhabitants of the hydrothermal anoxic basin. This difference did not explain the stratification of microbial communities in the different sediment layers of the brine-filled basin. A recent study showed that *Alcanivorax* was not present in all sediment layers of a sediment core from the Atlantis II basin [53]. A reasonable explanation for this finding is that the anhydrite layer at 177-198 cm in the sediment core was formed at a previous benthic site when hydrothermal solution was injected into the seafloor. The organisms living in the benthic water and subsurface sediment were subsequently sealed and protected in the anhydrite crystals. Because the metabolism of *A. borkumensis* bacteria was specifically used for the degradation of alkanes and other hydrocarbons in crude oil [51], the benthic site in which the anhydrite layer formed was probably an oil-spilling or oil-forming environment in the Atlantis II basin. The current hot sediments in the basin are biogenic and abiogenic sources of crude oil [54]. Seeping of the oil has resulted in proliferation of *A. borkumensis* bacteria in the bottom water. Similarly, oil-utilizing bacteria were nourished after the oil-spilling disaster in the Gulf of Mexico [55].

Based on the results in the present study, we postulated that mild eruptions of hydrothermal solutions injected calcium-rich solutions into the seafloor and produced anhydrite veins by mixing with sulfate in the bottom water of the Atlantis II rift basin. The anhydrite layer was then covered by sulfide minerals and biological debris such as the planktonic foraminifera *G. sacculifer*. In this study, we narrowed the age of the thick anhydrite layer to 750-770 years using ^{14}C isotope of the *G. sacculifer* specimens. This result also indicates a relatively young sediment age and a high accumulation rate of precipitated metals in the Atlantis II basin. Because the upward movement of hydrothermal solutions might transfer some foraminifera specimens from lower layers to the anhydrite layer, we did not use the foraminifera between anhydrite crystals. In our previous study, we have shown evidence of oil formation in the Atlantis II brine pool [50]. The organic carbon content can be converted to aromatic compounds under the hydrothermal conditions in the pool based on chemical

Biogeosciences Discuss., doi:10.5194/bg-2016-204, 2016
Manuscript under review for journal Biogeosciences
Published: 18 July 2016

and metagenomic evidence [50]. However, the bottom of the anoxic brine pool was not a habitat of *Alcanivorax* species [56,57], suggesting that *Alcanivorax* flourished in the basin before the formation of brine water layers over the sediment [57].

Although there were differences in microbial communities between the anhydrite crystals and the control sediment, *Ochrobactrum* sp. was one of the common inhabitants. Previous studies have shown that *Ochrobactrum* species could metabolize aromatic compounds aerobically and anaerobically [58,59], which explains their presence in both metagenomes assessed in the current study. Moreover, we determined the concentrations of nitrogen oxides in the different sulfide layers, although only low concentrations were detected. *Ochrobactrum* species were potentially able to anaerobically degrade polycyclic aromatic compounds using nitrate as an oxygen donor [59,60]. Such a chemolithoheterotrophic lifestyle is in accordance with the current *in situ* environment of the sediment in the Atlantis II. Regardless of the environmental changes indicated by the findings in the present study, the spreading of *Ochrobactrum* sp. was seemingly not affected. Although the metagenomes in the present study contained an abundant essential genes for degrading a variety of aromatic compounds, the microbial degradation of these compounds might have been attenuated by a lack of oxygen and a high level of salinity [61]. Anaerobic degradation of compounds is more difficult than aerobic degradation, often requiring oxygen donors such as nitrate and sulfate [59,60]. Based on its ability to survive under anoxic conditions, *Ochrobactrum* sp. is probably able to maintain a higher level of fitness in the control sediment compared with *Alcanivorax*. In the present study, the *Alkanindiges* identified in both metagenomes was also a well-known alkane degrader [62,63]. Because of its presence in both anhydrites and the adjacent sulfide layer, we assumed that the *Alkanindiges* bacterium was also capable of surviving aerobically and anaerobically in the oil-producing sediment. Hence, the change from an oxic to an anoxic benthic environment caused a dramatic shift in the microbial communities, resulting in the extinction of the obligate aerobic alkane-utilizer *Alcanivorax* and continuous residency of anaerobic oil-degraders. The availability of nitrogen oxides and the dissolution of sulfate from anhydrite crystals were possibly critical to the metabolic activities of the anaerobes. In addition, the *Bacillus* and fungi present in the control sediment were probably present in the form of dormant spores. In a recent report,

Biogeosciences Discuss., doi:10.5194/bg-2016-204, 2016
Manuscript under review for journal Biogeosciences
Published: 18 July 2016

Ochrobactrum and *Bacillus* were confirmed to be dominant species in some upper sulfide layers in the Atlantis II [53]. Altogether, in the present study, the current microbial inhabitants in the sulfide layers were largely different from those in the anhydrite crystals.

The geochemical data collected herein suggested that the sub-superficial anhydrite layer could release organic carbon contents into the sediment, as reported previously [12,13]. Our measurement of DOC at 80.9 mg L^{-1} in the anhydrite layer was higher than the generally accepted maximum value of 50 mg L^{-1} for marine sediments [64]. The abnormally high DOC was considered a notable alteration of the local environments, probably resulted from the breakdown of anhydrite crystals. Anhydrites in the Atlantis II brine sediment were likely maintained by the high salinity and temperature, and then slowly dissolved. This phenomenon may be explained by the slight undersatuation of the anhydrite in the Atlantis II sediment [17]. Such anhydrite layers are widely distributed in Middle Eastern sediments [65]. Hence, our findings shed light on the formation of micro-environments by anhydrite evaporites in the deep sediments. In this study, there was an inconsistency between the cell density and the DOC at the 12-cm depth layer, in which the DOC could not support a 10-fold higher biomass. This phenomenon probably resulted from the formation of petroleum compounds under the hydrothermal effects [50]. In the petroleum, hydrophobic organic compounds (HOCs) consisting of polycyclic aromatic hydrocarbons (PAHs) could not be counted in our DOC measurements (personal communication with J. Pearsons). The nutrient supply is critical for microbes to survive in deep-sea sediment. Apart from the chemolithoautotrophic microbes, numerous other inhabitants take advantage of the buried organic matter. Importantly, the trapped organic matter serves as a nutrient supply following the dissolution of organic-rich anhydrite crystals. Therefore, our findings highlighted the importance of the nutrients released from the anhydrite facies for microbes in deep-sea subsuperficial sediment.

Author contributions. Y. Wang, T.G. Li, and P. Y. Qian were responsible for the study design. Data analysis was performed by Y. Wang, T.G. Li, J. T. Li, Q. L. Lai, and Z. M. Gao. M.Y. Wang conducted FISH assay. The manuscript was prepared by Y. Wang with contributions from all co-authors.

Biogeosciences Discuss., doi:10.5194/bg-2016-204, 2016
Manuscript under review for journal Biogeosciences
Published: 18 July 2016

Acknowledgments. This study was supported by the National Science Foundation of China No. 41476104 and No. 31460001, the National Basic Research Program of China (973 Program, No. 2012CB417304), and the King Abdullah University of Science and Technology (SA-C0040/UK-C0016) to P.Y. Qian. This work was also supported by the Strategic Priority Research Program of the Chinese Academy of Sciences (XDB06010102 and XDB06010201).

References

1 Orcutt, B. N., Sylvan, J. B., Knab, N. J. & Edwards, K. J. Microbial ecology of the dark ocean above, at, and below the seafloor. *Microbiol Mol Biol Rev* **75**, 361-422, doi:Doi 10.1128/Mmbr.00039-10 (2011).

2 Teske, A. & Sorensen, K. B. Uncultured archaea in deep marine subsurface sediments: have we caught them all? *ISME J* **2**, 3-18 (2007).

3 Parkes, R. J., Cragg, B. A. & Wellsbury, P. Recent studies on bacterial populations and processes in subseafloor sediments: A review. *Hydrogeol J* **8**, 11-28, doi:10.1007/pl00010971 (2000).

4 Webster, G. *et al.* Prokaryotic community composition and biogeochemical processes in deep subseafloor sediments from the Peru Margin. *FEMS Microbiol Ecol* **58**, 65-85, doi:10.1111/j.1574-6941.2006.00147.x (2006).

5 Brocks, J. J. *et al.* Biomarker evidence for green and purple sulphur bacteria in a stratified Palaeoproterozoic sea. *Nature* **437**, 866-870, (2005).

6 Hill, A. E. The transition temperature of gypsum to anhydrite. *J Am Chem Soc* **59**, 2242-2244, doi:10.1021/ja01290a039 (1937).

7 Dupraz, C., Reid, R. P. & Visscher, P. T. in *Encyclopaedia of Geobiology* (eds V. Reitner & J. Thiel) 617-635 (Springer, 2011).

8 Petrash, D. A. *et al.* Dynamic controls on accretion and lithification of modern gypsum-dominated thrombolites, Los Roques, Venezuela. *Sedi Geol* **245-246**, 29-47 (2012).

9 Trichet, J., Défarge, C., Tribble, J., Tribble, G. W. & Sansone, F. J. Christmas Island lagoonal lakes, models for the deposition of carbonate-evaporite-organic laminated sediments. *Sedi Geol* **140**, 177-189 (2001).

10 Babel, M. Models for evaporite, selenite and gypsum microbialite deposition in ancient saline basins. *Acta Geologica Polonica* **54**, 219-249 (2004).

11 Jannasch, H. W. & Mottl, M. J. Geomicrobiology of deep-sea hydrothermal vents. *Science* **229**, 717-725, doi:10.1126/science.229.4715.717 (1985).

12 Kristall, B., Kelley, D. S., Hannington, M. D. & Delaney, J. R. Growth history of a diffusely venting sulfide structure from the Juan de Fuca Ridge: A petrological and geochemical study. *Geochem. Geophys. Geosyst.* **7**, Q07001, doi:10.1029/2005gc001166 (2006).

13 Swallow, J. C. & Crease, J. Hot salty water at the bottom of the Red Sea. *Nature* **205**, 165-166 (1965).

14 Girdler, R. W. A review of Red Sea heat flow. *Phil Trans Roy Soc Lon A* **267**, 191-203 (1970).

15 Anschutz, P. & Blanc, G. Heat and salt fluxes in the Atlantis II Deep (Red Sea). *Earth Planet Sci Lett* **142**, 147-159 (1996).

16 Shipboard Scientific Party in *Deep Sea Drilling Project* **23**, 595-600 (1974).

17 Anschutz, P., Blanc, G., Monnin, C. & Boulègue, J. Geochemical dynamics of the Atlantis II Deep (Red Sea): II. Composition of metalliferous sediment pore waters. *Geochim Cosm Acta* **64**, 3995-4006 (2000).

18 Ramboz, C., Oudin, E. & Thisse, Y. Geyser-type discharge in Atlantis II Deep, Red Sea: evidence of boiling from fluid inclusions in epigenetic anhydrite. *Can Mineral* **26**, 765-786 (1988).

19 Zierenberg, R. A. & Shanks, W. C. Mineralogy and geochemistry of epigenetic features in metalliferous sediment, Atlantis II Deep, Red Sea. *Econ Geol* **78**, 57-72, doi:10.2113/gsecongeo.78.1.57 (1983).

20 Oudin, E., Thisse, Y. & Ramboz, C. Fluid inclusion and mineralogical evidence for high temperature saline hydrothermal circulation in the Red Sea metalliferous sediments: preliminary results. *Mar. Mining* **5**, 3-31 (1984).

21 Missack, E., Stoffers, P. & El Goresy, A. Mineralogy, paragenesis, and phases relations of copper iron sulfides in the Atlantis II Deep, Red Sea. *Min. Deposita* **24**, 82-91 (1989).

22 Bower, A. S. R/V Oceanus Voyage 449-6 Red Sea Atlantis II Deep Complex Area 19 October-1 November 2008. (Woods Hole Oceanographic Institution, 2009).

23 Gough, H. L. & Stahl, D. A. Optimization of direct cell counting in sediment. *J Microbiol Methods* **52**, 39-46 (2003).

24 Reimer, P. J. *et al.* IntCal09 and Marine09 radiocarbon age calibration curves, 0-50,000yeats cal BP. *Radiocarbon* **51**, 1111-1150 (2009).

25 Bard, E. Correction of accelerator mass spectrometry 14C ages measured in planktonic foraminifera: Paleoceanographic implications. *Paleoceanography* **3**, 635-645 (1988).

26 Zong, C., Lu, S., Chapman, A. R. & Xie, X. S. Genome-wide detection of single-nucleotide and copy-number variations of a single human cell. *Science* **338**, 1622-1626, doi:10.1126/science.1229164 (2012).

27 Wang, Y. *et al.* An evaluation of multiple annealing and looping based genome amplification using a synthetic bacterial community. *ACTA Oceanol Sin* **35**, 131-136 (2016).

28 Nurk, S. *et al.* Assembling single-cell genomes and mini-metagenomes from chimeric MDA products. *J Comput Biol* **20**, 714-737, doi:10.1089/cmb.2013.0084 (2013).

29 Li, H. *et al.* The sequence alignment/map format and SAMtools. *Bioinformatics* **25**, 2078-2079, doi:DOI 10.1093/bioinformatics/btp352 (2009).

30 Huang, Y., Gilna, P. & Li, W. Identification of ribosomal RNA genes in metagenomic fragments. *Bioinformatics* **25**, 1338-1340 (2009).

31 Albertsen, M. *et al.* Genome sequences of rare, uncultured bacteria obtained by differential coverage binning of multiple metagenomes. *Nat Biotechnol* **31**, 533-535, doi:Doi 10.1038/Nbt.2579 (2013).

32 Hyatt, D. *et al.* Prodigal: prokaryotic gene recognition and translation initiation site identification. *BMC Bioinformatics* **11**, doi:Artn 119 Doi 10.1186/1471-2105-11-119 (2010).

33 Kanehisa, M., Goto, S., Sato, Y., Furumichi, M. & Tanabe, M. KEGG for integration and interpretation of large-scale molecular data sets. *Nucleic Acids Res* **40**, D109-114, doi:10.1093/nar/gkr988 gkr988 [pii] (2012).

34 Overbeek, R. *et al.* The subsystems approach to genome annotation and its use in the project to annotate 1000 genomes. *Nucleic Acids Res* **33**, 5691-5702, doi:33/17/5691 [pii]10.1093/nar/gki866 (2005).

35 Goris, J. *et al.* DNA–DNA hybridization values and their relationship to whole-genome sequence similarities. *Int J Syst Evol Microbiol* **57**, 81-91 (2007).

36 Meier-Kolthoff, J. P., Auch, A. F., Klenk, H. P. & Goker, M. Genome sequence-based species delimitation with confidence intervals and improved distance functions. *BMC Bioinformatics* **14**, 60, doi:10.1186/1471-2105-14-60 (2013).

37 Auch, A. F., Klenk, H. P. & Goker, M. Standard operating procedure for calculating genome-to-genome distances based on high-scoring segment pairs. *Stand Genomic Sci* **2**, 142-148, doi:10.4056/sigs.541628 (2010).

38 Auch, A. F., von Jan, M., Klenk, H. P. & Goker, M. Digital DNA-DNA hybridization for microbial species delineation by means of genome-to-genome sequence comparison. *Stand Genomic Sci* **2**, 117-134, doi:10.4056/sigs.531120 (2010).

39 Kim, O. S. *et al.* Introducing EzTaxon-e: a prokaryotic 16S rRNA gene sequence database with phylotypes that represent uncultured species. *Int J Syst Evol Microbiol* **62**, 716-721, doi:10.1099/ijs.0.038075-0 (2012).

40 Tamura, K. *et al.* MEGA5: molecular evolutionary genetics analysis using maximum likelihood, evolutionary distance, and maximum parsimony methods. *Mol Biol Evol* **28**, 2731-2739 (2011).

41 Ludwig, W. *et al.* ARB: a software environment for sequence data. *Nucl. Acids Res.* **32**, 1363-1371, doi:10.1093/nar/gkh293 (2004).

42 Quast, C. *et al.* The SILVA ribosomal RNA gene database project: improved data processing and web-based tools. *Nucl Acids Res* **41**, D590-D596, doi:10.1093/nar/gks1219 (2013).

43 Wang, W., Wang, L. & Shao, Z. Diversity and abundance of oil-degrading bacteria and alkane hydroxylase (alkB) genes in the subtropical seawater of Xiamen Island. *Microb Ecol* **60**, 429-439, doi:10.1007/s00248-010-9724-4 (2010).

44 Pernthaler, A., Pernthaler, J. & Amann, R. Fluorescence in situ hybridization and catalyzed reporter deposition for the identification of marine bacteria. *Appl Environ Microb* **68**, 3094-3101 (2002).

45 Barret, M. *et al.* Methanoculleus spp. as a biomarker of methanogenic activity in swine manure storage tanks. *FEMS Microbiol Ecol* **80**, 427-440, doi:10.1111/j.1574-6941.2012.01308.x (2012).

46 Schneiker, S. *et al.* Genome sequence of the ubiquitous hydrocarbon-degrading marine bacterium Alcanivorax borkumensis. *Nature Biotechnol* **24**, 997-1004, doi:10.1038/nbt1232 (2006).

47 Sabirova, J. S. *et al.* Transcriptional profiling of the marine oil-degrading bacterium Alcanivorax borkumensis during growth on n-alkanes. *FEMS Microbiol Lett* **319**, 160-168, doi:10.1111/j.1574-6968.2011.02279.x (2011).

48 Wayne, L. G. *et al.* Report of the ad hoc committee on reconciliation of approaches to bacterial systematics. *Int J Syst Evol Microbiol* **37**, 463-464 (1987).

49 Richter, M. & Rossello-Mora, R. Shifting the genomic gold standard for the prokaryotic species definition. *Proc Natl Acad Sci U S A* **106**, 19126-19131, doi:10.1073/pnas.0906412106 (2009).

50 Wang, Y. *et al.* Hydrothermally generated aromatic compounds are consumed by bacteria colonizing in Atlantis II Deep of the Red Sea. *ISME J* **5**, 1652–1659 (2011).

51 Yakimov, M. M., Timmis, K. N. & Golyshin, P. N. Obligate oil-degrading marine bacteria. *Curr Opin Biotech* **18**, 257-266, doi:http://dx.doi.org/10.1016/j.copbio.2007.04.006 (2007).

52 Bougouffa, S. *et al.* Distinctive microbial community structure in highly stratified deep-sea brine water columns. *Appl Environ Microb* **79**, 3425-3437, doi:Doi 10.1128/Aem.00254-13 (2013).

53 Wang, Y. *et al.* Zonation of Microbial Communities by a Hydrothermal Mound in the Atlantis II Deep (the Red Sea). *PLoS ONE* **10**, e0140766, doi:10.1371/journal.pone.0140766 (2015).

54 Simoneit, B. R. T. Petroleum generation submarine hydrothermal systems: An update. *Can Mineral* **26**, 827-840 (1988).

55 Gutierrez, T. *et al.* Hydrocarbon-degrading bacteria enriched by the Deepwater Horizon oil spill identified by cultivation and DNA-SIP. *ISME J* **7**, 2091-2104, doi:10.1038/ismej.2013.98 (2013).

56 Bougouffa, S. *et al.* Distinctive microbial community structure in highly stratified deep-sea brine water columns. *Appl Environ Microb* **79**, 3425-3437, doi:10.1128/AEM.00254-13 (2013).

57 Blanc, G. & Anschutz, P. New stratification in the hydrothermal brine system of the Atlantis II Deep, Red Sea. *Geology* **23**, 543-546, (1995).

58 Zu, L., Xiong, J., Li, G., Fang, Y. & An, T. Concurrent degradation of tetrabromobisphenol A by Ochrobactrum sp. T under aerobic condition and estrogenic transition during these processes. *Ecotoxicol Environ Safety* **104**, 220-225, doi:10.1016/j.ecoenv.2014.03.015 (2014).

59 Mahmood, Q. *et al.* Isolation of Ochrobactrum sp.QZ2 from sulfide and nitrite treatment system. *J Hazardous Materials* **165**, 558-565, doi:http://dx.doi.org/10.1016/j.jhazmat.2008.10.021 (2009).

60 Wu, Y. *et al.* Isolation of marine benzo[a]pyrene-degrading Ochrobactrum sp. BAP5 and proteins characterization. *J Environ Sci* **21**, 1446-1451, (2009).

61 Klinkhammer, G. P. & Lambert, C. E. Preservation of organic matter during salinity excursions. *Nature* **339**, 271-274 (1989).

62 Klein, A. N., Frigon, D. & Raskin, L. Populations related to Alkanindiges, a novel genus containing obligate alkane degraders, are implicated in biological foaming in activated sludge systems. *Environ Microbiol* **9**, 1898-1912, (2007).

63 Bogan, B. W. *et al.* Alkanindiges illinoisensis gen. nov., sp. nov., an obligately hydrocarbonoclastic, aerobic squalane-degrading bacterium isolated from oilfield soils. *Int J Syst Evol Microbiol* **53**, 1389-1395, doi:10.1099/ijs.0.02568-0 (2003).

64 Cameron, D., Willett, M. & Hammer, L. Distribution of organic carbon in the Berkeley Pit lake, Butte, Montana. *Mine Water Environ* **25**, 93-99, (2006).

65 Alsharhan, A. S. & Nairn, A. E. M. *Sedimentary basins and petroleum geology of the Middle East*. (Elsevier Science B.V., 1997).

Biogeosciences Discuss., doi:10.5194/bg-2016-204, 2016
Manuscript under review for journal Biogeosciences
Published: 18 July 2016

Data Accessibility

Illumina raw data will be accessible under SRA356974 in the NCBI SRA database. *B. borkumensis* ABS183 genome was deposited in the NCBI under BioProject LKAP00000000 and will be public on October 31, 2016.

Table 1. Age estimates of the sediment layers

Layer (cm)	Age (year)	Age error (year)
3-6	320	25
21-24	475	35
45-48	490	30
90-93	500	25
129-132	560	35
153-156	750	30
198-201	770	30
222-225	880	30

Eight sediment layers were selected for the age estimates using radioisotope ^{14}C of *G. sacculifer* collected from the respective layers. The age was corrected by the 400-year reservoir age with an error range.

Biogeosciences Discuss., doi:10.5194/bg-2016-204, 2016
Manuscript under review for journal Biogeosciences
Published: 18 July 2016

Figures

Figure 1. Anhydrite crystals and genome binning.

Anhydrite crystals in a Petri dish (90 mm in diameter) (A) were used for DNA extraction. The amplified genomic DNA was sequenced and then reassembled. Based on the G+C content and read coverage, the binned contigs with high coverage levels (B) were selected for examination of the tetranucleotide frequency consistency in the PCA analysis (C).

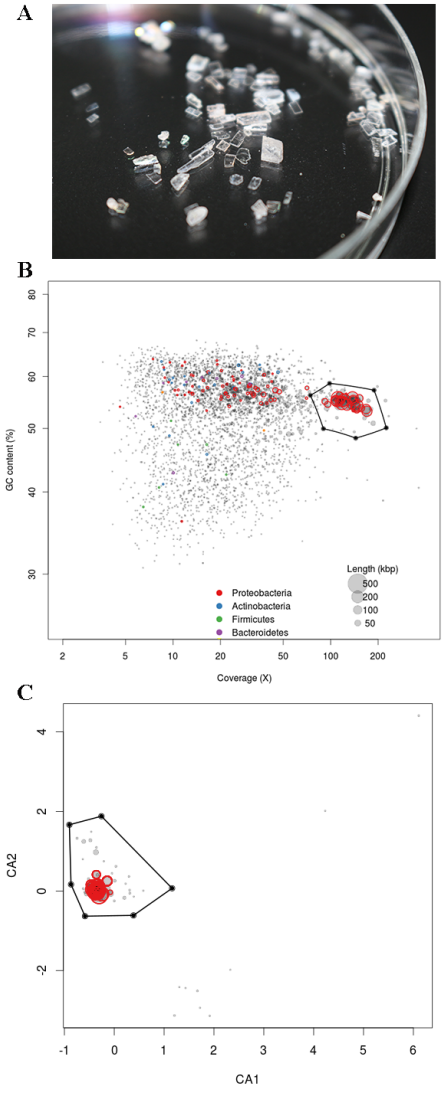

Biogeosciences Discuss., doi:10.5194/bg-2016-204, 2016
Manuscript under review for journal Biogeosciences
Published: 18 July 2016

Figure 2. Nutrient measurements and cell counts in the different sediment layers. The pore water samples were analyzed for five layers of a sediment core obtained from the Atlantis II Deep (21°20.76' N, 38°04.68' E) in 2008. DOC: dissolved organic carbon.

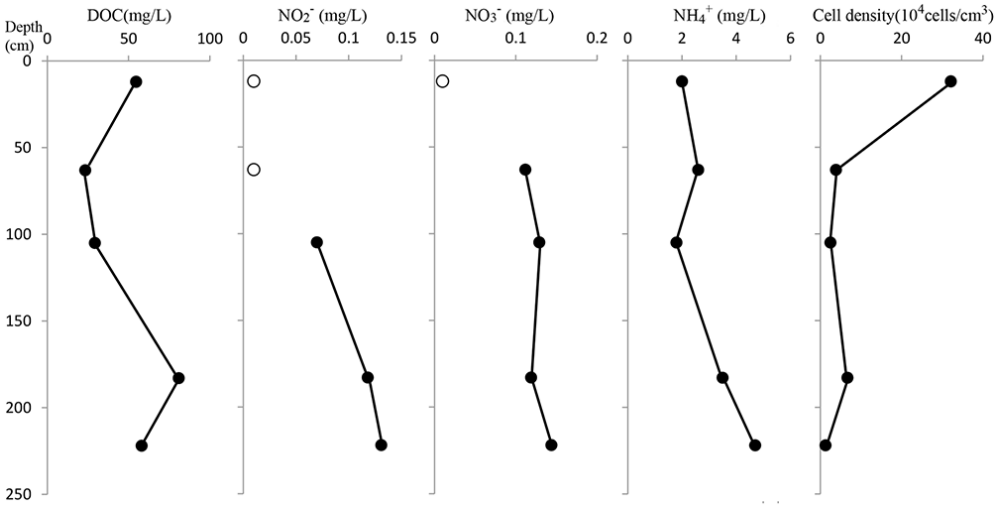

Biogeosciences Discuss., doi:10.5194/bg-2016-204, 2016
Manuscript under review for journal Biogeosciences
Published: 18 July 2016

Figure 3 Grain size and age of selected layers

The percentages of the small particles (<63µm) in dry weight are shown for 75 slices of the sediment core (small squares on the line). The age estimates (black circles) of the selected layers were performed using radioisotope 14C of the monospecific *Globigerinoides sacculifer* specimens. Age errors ranged between 25 to 40 years. Anhydrite and control layers for metagenomic study were indicated by arrows.

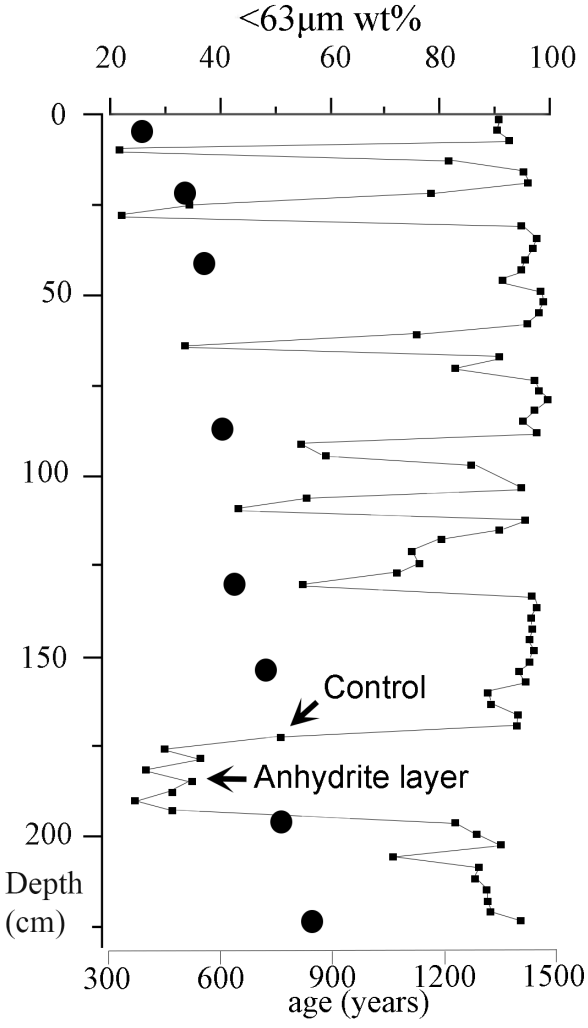

Biogeosciences Discuss., doi:10.5194/bg-2016-204, 2016
Manuscript under review for journal Biogeosciences
Published: 18 July 2016

Figure 4. Microbial communities in anhydrite crystals and neighboring control sediment.

Phyla and genera in the anhydrite crystals and control layer were predicted using 16S/18S rRNA gene fragments extracted from the corresponding metagenomes (D-T: Deinococcus-Thermus). The relative abundance of the genera can be estimated by the coverage level of the 16S/18S rRNA fragments by reads.

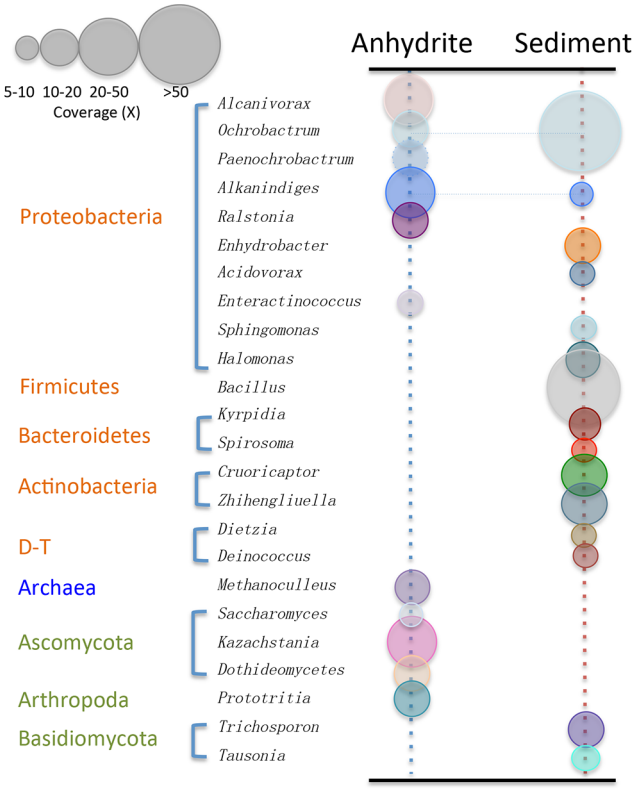

Biogeosciences Discuss., doi:10.5194/bg-2016-204, 2016
Manuscript under review for journal Biogeosciences
Published: 18 July 2016

Figure 5. Phylogenetic tree of 16S rRNA genes.

Bootstrap values (expressed as percentages of 1000 replications) are shown at the branches of the neighbor-joining tree.

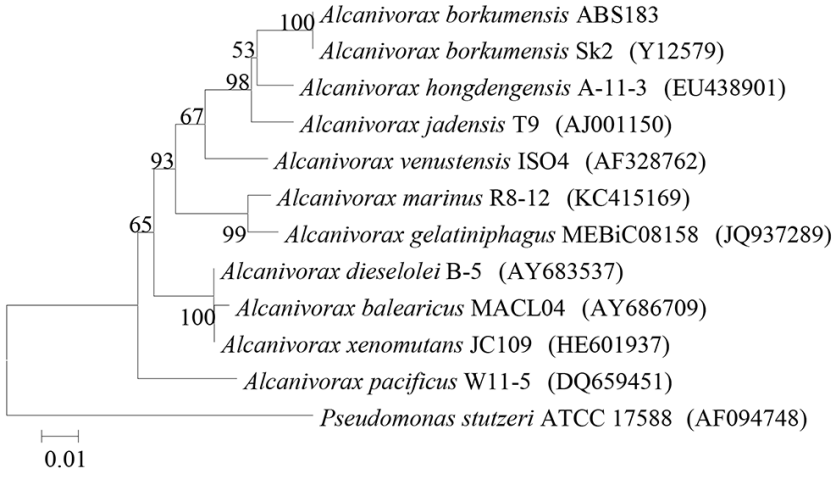

Biogeosciences Discuss., doi:10.5194/bg-2016-204, 2016
Manuscript under review for journal Biogeosciences
Published: 18 July 2016

Figure 6. Fluorescence *in situ* hybridization (FISH) of *Alcanivorax* sp. ABS183 embedded in anhydrite crystals.

DAPI staining and FISH using 16S rRNA probes are shown in A and B. The merged image of A and B is shown in Fig. 6C. DAPI staining and FISH were also performed using two samples that were filtered with 3-µm (D-G) and 0.22-µm (H-K) membranes, respectively. *Alcanivorax* bacteria were released from the large crystals filtered through the 3-µm membranes (D-G). The bacteria were stained with DAPI (D), 16S rRNA probes (E) and the *alkB* probe (F), respectively, and overlaid (G). Using a sample filtered through a 0.22-µm membrane, a dividing *Alcanivorax* sp. ABS183 cell was labeled using the same method and probes (H-J). The microscopic fields shown in H-J are merged in Fig. 6K.